

Five-Dimensional Fission-Barrier Calculations from ^{70}Se to ^{252}Cf

Peter MÖLLER^{1,*}, Arnold J. SIERK¹, and Akira IWAMOTO²

¹*Theoretical Division, Los Alamos National Laboratory, Los Alamos, New Mexico 87545, USA*

²*Japan Atomic Energy Research Institute, Tokai-mura, Naka-gun, Ibaraki, 319-1195 Japan*

(Dated: October 29, 2018)

We present fission-barrier-height calculations for nuclei throughout the Periodic Table based on a realistic macroscopic-microscopic model. Compared to other calculations: (1) we use a deformation space of a sufficiently high dimension, sampled densely enough to describe the relevant topography of the fission potential, (2) we unambiguously find the physically relevant saddle points in this space, and (3) we formulate our model so that we obtain continuity of the potential energy at the division point between a single system and separated fission fragments or colliding nuclei, allowing us to (4) describe both fission-barrier heights and ground-state masses throughout the Periodic Table.

PACS numbers: 24.75.+i, 25.85.-w, 21.10.Dr, 25.70.Gh, 21.60.Cs, 21.10.Sf

It has been notoriously difficult to calculate in a consistent theoretical model with microscopic content both fission barriers and ground-state masses for nuclei throughout the Periodic Table. So far this has only been possible in the framework of a macroscopic-microscopic model [1, 2]. However, developments in the area of nuclear fission show that these earlier studies can now be improved.

On the experimental side it became clear that the barrier data for the two lightest nuclei previously used in the determination of model constants are incorrect. In addition, a series of measurements of fission-barrier heights of nuclei with atomic numbers in the neighborhood of $A = 100$ are now available [3, 4, 5]. Barrier heights calculated for these light nuclei using the model from Ref. [1] are from 1 to 5 MeV too low [6, 7].

On the theoretical side we have recently shown that five-dimensional deformation spaces with the potential energy defined on millions of points are necessary to determine properly the details of the potential energy such as the locations and heights of the fission saddle points [8, 9]. This large deformation space is in stark contrast to one with three degrees of freedom and 175 deformation points previously used to determine the locations and heights of saddle points [1, 2]. Moreover, it has been clear for some time that the Wigner and A^0 macroscopic terms in these nuclear mass models must have a shape dependence [10]. This was ignored in previous global calculations [1, 2, 6, 7] and only incorporated in some of our more limited fission-barrier studies, for example [11].

In nuclear fission the nucleus evolves from a single ground-state shape into two separated fission fragments. During the shape and configuration changes that occur in this process the total energy of the system initially increases up to a maximum, the fission-barrier height, then decreases. Calculations of fission barriers involve the determination of the total nuclear potential energy

for different nuclear shapes. Such a calculation defines an energy landscape as a function of a number of shape coordinates. The fission-barrier height is given by the energy relative to the ground state of the most favorable saddle point that has to be traversed when the shape evolves from a single shape to separated fragments. We use a technique borrowed from the area of geographical topography studies, namely immersion (“imaginary water flow”) [12, 13, 14], to determine the structure of the high-dimensional fission potential-energy surfaces [8, 9].

A number of models exist for the nuclear potential energy. At first sight, it would seem attractive to employ a self-consistent mean-field (SMF) model using effective forces, for example a Hartree-Fock (HF) or Hartree-Fock-Bogolyubov (HFB) model with Skyrme or Gogny effective interactions [15, 16, 17], or a relativistic Dirac-Hartree model with scalar and vector interactions [18]. Global HF mass calculations have recently been presented [19, 20]. However, at least two major problems with such calculations remain unresolved. First, no effective force has been found which can describe both nuclear masses and fission barriers for nuclei of all mass numbers. Second, even if an appropriate effective interaction could be determined, it is extremely difficult, and in practice has so far proven impossible unambiguously to locate an actual saddle-point configuration in SMF models. There exists a common misconception that constrained self-consistent HF or HFB calculations with Skyrme or Gogny forces automatically take into account all non-constrained shape variables in a proper manner. In fact, the apparent saddle points that appear in constrained HF calculations in the general case have no relation to the true saddle points; we give an illustrative example below.

For calculating the fission potential-energy surface in this work, we adopt the macroscopic-microscopic finite-range liquid-drop model (FRLDM) [2] generalized to account for all required shape-dependencies of its various macroscopic terms. In contrast the finite-range droplet model (FRDM) [2] cannot be generalized in this way. In Fig. 1 we illustrate the large discontinuities that occur at the transition point between single and separated sys-

*Electronic address: moller@moller.lanl.gov

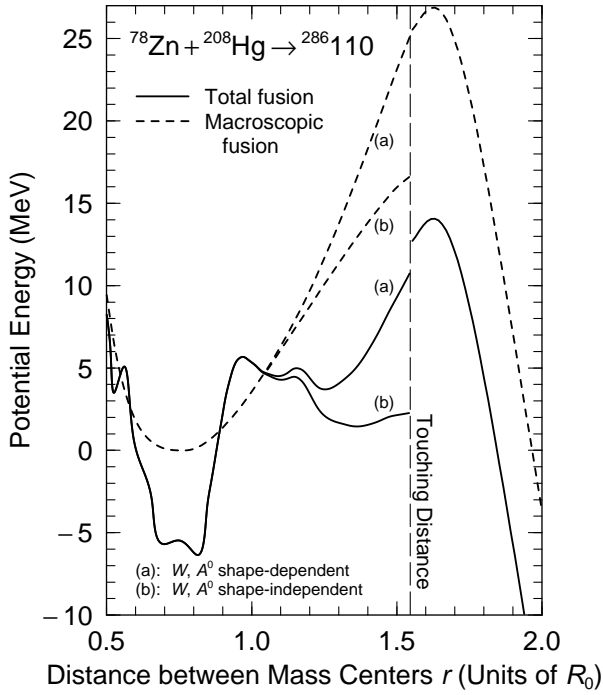


FIG. 1: Calculated macroscopic and total potential energies, for shape sequences leading to the touching configuration, at the long-dashed line, of spherical ^{78}Zn and ^{208}Hg . To the left the calculations trace the energy for a *single, joined* shape configuration from oblate shapes through the spherical shape at $r = 0.75$ to the touching configuration at $r = 1.52$; to the right the calculations trace the energy for separated spherical nuclei beyond the touching point. The continuous path through five-dimensional space from the ground state to the touching configuration is arbitrary; the key point is that the limiting shapes when approaching the line of touching from the left and right are identical, namely spherical ^{78}Zn and ^{208}Hg in contact. At a specific value of r all curves are calculated for the same shape. To obtain continuity of the macroscopic energy at touching, a crucial feature in realistic models, it is essential that various model terms depend appropriately on nuclear shape, as is the case for the curves (a). The slight remaining discontinuity in the *total* fusion energy curve arises because the Fermi surfaces of the nuclei readjust at touching, and because pairing and spin-orbit strength parameters also undergo small discontinuous changes there.

tems when the shape dependences of the Wigner and A^0 macroscopic energies are neglected, and the continuous behavior exhibited for the current formulation.

In the macroscopic-microscopic approach, it is important that the shape description be flexible enough to allow accessing those configurations which are physically important to the fission process. In addition to the commonly used elongation, necking and mass-asymmetry degrees of freedom, it is essential to include the deformations of the partially formed fragments. This is because the microscopic binding due to fragment shell structure, which is sensitive to the fragment deformations, can be

as large as 5 MeV even for shapes with a fairly large neck radius. We use the three-quadratic-surface (3QS) shape parameterization [9, 21] to describe shapes with these five degrees of freedom. By investigating the scale over which the microscopic energy varies significantly, we determine the coordinate mesh upon which we need to define the energy. We find that we get a reasonable coverage of the space by defining a grid of 15 points each in the neck diameter and left and right fragment deformations, 20 points in the mass asymmetry, and 41 points in the nuclear elongation. A few grid points do not refer to real shapes, so we are left with a grid of 2,610,885 points [9].

In an unconstrained mean-field calculation, one starts with some initial density, usually defined in terms of trial wavefunctions, then determines new wavefunctions which are solutions of the potential derived from the density. By iterating to convergence one finds a local minimum: the nuclear ground state or possibly a fission-isomeric state. To try to find a fission barrier, some have chosen to solve a constrained problem, which leads to the minimum-energy state subject to the constraint, often taken to be the quadrupole moment. By applying a series of constraints with increasing deformation, a curve of energy as a function of constrained deformation is found. Such curves often exhibit discontinuities and may not pass through the real saddle point in multidimensional space as is discussed in more detail in Refs. [8, 22].

In a macroscopic-microscopic calculation one should in principle be able to locate saddle points by solving for all shapes that have a zero derivative of the energy with respect to all the degrees of freedom. This method works for a purely macroscopic model [7], but macroscopic-microscopic models using the Strutinsky shell-correction technique [23, 24], are subject to fluctuations when small shape changes are made, making it difficult to obtain accurate derivatives by numerical techniques. Even if all saddle points in a high-dimensional space could be found in this way, one must still understand the topography and deduce which saddle would correspond to the actual peak of the barrier. Before the breakthrough study in Ref. [13], what has usually been done in calculations involving more than two degrees of freedom is to first define a two-dimensional space of two primary shape coordinates. For each point in this two-dimensional space the energy is then minimized with respect to a set of additional shape degrees of freedom. It was incorrectly assumed that if no discontinuities occurred in this two-dimensional surface then its saddle points would be identical to the saddle-points in the full, higher-dimensional space. For all but the most structureless functions this procedure is incorrect and may actually result in more inaccurate saddle points than if only the original two-dimensional space is studied.

We illustrate in Fig. 2 some of the problems that one may encounter in either a constrained SMF calculation or in a macroscopic-microscopic model when attempting to reduce the dimensionality of a problem via minimization while preserving the essential features of the potential

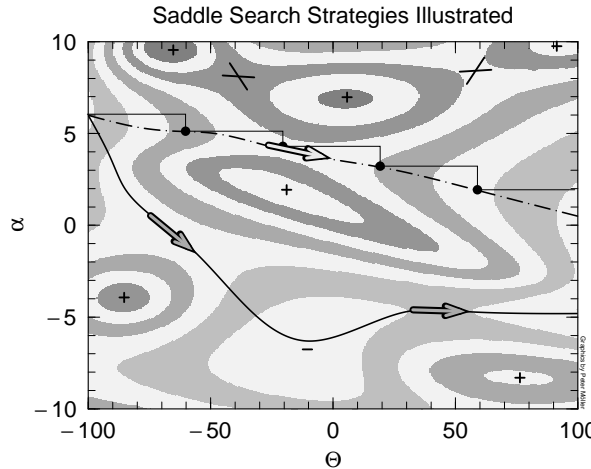


FIG. 2: Maxima (+), minima (−), and saddle points (arrows or crossed lines) of a two-dimensional function. As discussed in the text it is not possible to obtain a lower-dimensional representation of this surface by “minimizing” with respect to the “additional” (α) shape degree of freedom. Darker shades of gray indicate higher function values. Alternate contour bands are light gray for readability.

energy. We assume the Θ coordinate corresponds to the fission direction and α to all other degrees of freedom. Because of the multiple saddle points, it is not clear *a priori* which one would correspond to the fission threshold. We identify the point $\Theta = -100$, $\alpha = 6$ as the ground state or fission-isomer state and proceed to find a “constrained” fission barrier. From the starting point we increase Θ by 40 (smaller steps will not alter the result) while keeping α fixed. From the new position we then minimize with respect to α and find ourselves at the first black dot. When we repeat this process we obtain the dot-dashed curve. The energy along this path is a continuous function and the white arrow would be identified as the fission saddle point. However, this saddle is higher than those shown by gray arrows, which can only be identified when the full space is explored. Of course in a constrained SMF calculation the convergence towards a solution is more complex than “sliding downhill”, since the wave functions and potential change during this process. However, solutions of constrained SMF equations do show similar behavior; often converging to a local minimum which depends on the starting configuration, a process similar to what is sketched in Fig. 2.

The fundamental point is that the fission saddle point can only be determined from global properties of the multidimensional energy surface, not from local excursions from a specific starting point. We therefore implement the immersion method mentioned above and first identify all minima by locating the points which have a lower energy than all $3^n - 1$ neighboring points in n -dimensional coordinate space. We then progressively fill

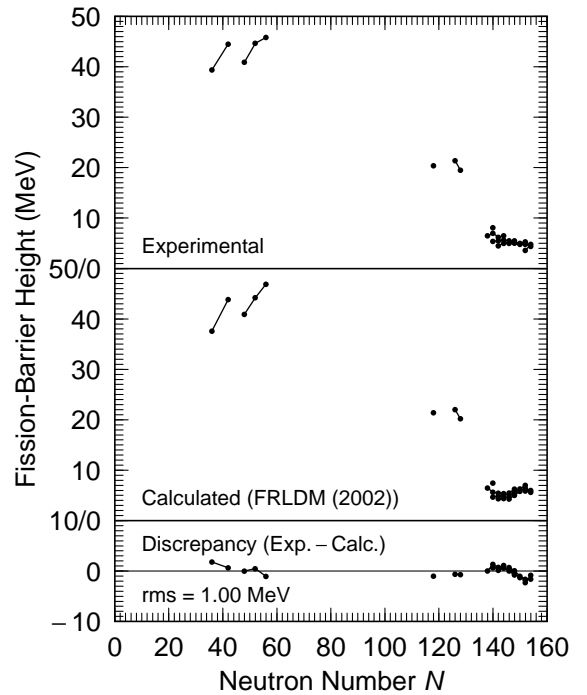


FIG. 3: Comparison of calculated and experimental fission-barrier heights for nuclei throughout the Periodic Table, after a readjustment of the macroscopic model constants. Experimental barriers are well reproduced by the calculations, the rms error is only 0.999 MeV for 31 nuclei. In the actinide region it is the outer of the two peaks in the “double-humped” barrier that is compared to experimental data.

up the ground-state minimum with “water”, determining when a prespecified point in the fission valley becomes “wet”. By adjusting the increase in the water level carefully we are able unambiguously to identify the location and energy of the grid point nearest to the true saddle.

Because we are studying a higher dimensional deformation space with over 10000 times as many points as in previous calculations, we find that the saddles for a given nucleus are always lower than those found for the same model parameters in our earlier studies [2, 8]. This means we need to redetermine the parameters of our

TABLE I: Macroscopic model parameters of the FRLDM (1992) and those obtained in the present adjustment, designated FRLDM (2002) using barrier heights obtained in our five-dimensional calculation.

| Constant | FRLDM (1992) | FRLDM (2002) |
|------------|--------------|--------------|
| a_v | 16.00126 MeV | 16.02500 MeV |
| κ_v | 1.92240 MeV | 1.93200 MeV |
| a_s | 21.18466 MeV | 21.33000 MeV |
| κ_s | 2.34500 MeV | 2.37800 MeV |
| a_0 | 2.61500 MeV | 2.04000 MeV |
| c_a | 0.10289 MeV | 0.09700 MeV |

TABLE II: Calculated barriers for 31 nuclei compared to experimental data. The first 5 barriers are macroscopic barriers.

| <i>Z</i> | <i>A</i> | E_{exp} (MeV) | E_{calc} (MeV) | ΔE (MeV) | <i>Z</i> | <i>A</i> | E_{exp} (MeV) | E_{calc} (MeV) | ΔE (MeV) |
|----------|----------|---------------------------|----------------------------|---------------------|----------|----------|---------------------------|----------------------------|---------------------|
| 34 | 70 | 39.40 | 37.58 | 1.81 | 92 | 238 | 5.50 | 5.48 | 0.01 |
| 34 | 76 | 44.50 | 43.84 | 0.65 | 92 | 240 | 5.50 | 6.27 | -0.77 |
| 42 | 90 | 40.92 | 40.92 | -0.00 | 94 | 236 | 4.50 | 4.35 | 0.14 |
| 42 | 94 | 44.68 | 44.20 | 0.47 | 94 | 238 | 5.00 | 4.39 | 0.60 |
| 42 | 98 | 45.84 | 46.88 | -1.04 | 94 | 240 | 5.15 | 4.83 | 0.31 |
| 80 | 198 | 20.40 | 21.41 | -1.01 | 94 | 242 | 5.05 | 5.55 | -0.50 |
| 84 | 210 | 21.40 | 22.02 | -0.62 | 94 | 244 | 5.00 | 6.29 | -1.29 |
| 84 | 212 | 19.50 | 20.20 | -0.70 | 94 | 246 | 5.30 | 7.01 | -1.71 |
| 88 | 228 | 8.10 | 7.45 | 0.64 | 96 | 242 | 5.00 | 4.28 | 0.71 |
| 90 | 228 | 6.50 | 6.47 | 0.02 | 96 | 244 | 5.10 | 5.02 | 0.07 |
| 90 | 230 | 7.00 | 5.65 | 1.34 | 96 | 246 | 4.80 | 5.81 | -1.01 |
| 90 | 232 | 6.20 | 5.45 | 0.74 | 96 | 248 | 4.80 | 6.41 | -1.61 |
| 90 | 234 | 6.50 | 5.36 | 1.13 | 96 | 250 | 4.40 | 5.98 | -1.58 |
| 92 | 232 | 5.40 | 4.67 | 0.72 | 98 | 250 | 3.60 | 5.88 | -2.28 |
| 92 | 234 | 5.50 | 4.89 | 0.60 | 98 | 252 | 4.80 | 5.63 | -0.83 |
| 92 | 236 | 5.67 | 4.98 | 0.68 | | | | | |

nuclear-structure model. Because new parameter sets may change the location of the saddle points and minima, an iterative procedure is in principle required. However these changes in deformation are small; here we do just the first iteration and vary six parameters of the macroscopic energy functional to optimize the reproduction of both ground-state binding energies and fission-barrier heights. This process is identical to the one followed in

the creation of our 1995 mass table [2]. We show in Table I the constants from Ref. [2] (determined in 1992) and those obtained in our readjustment taking into account the larger deformation space in locating the fission saddle points. We have made a number of tests which allow us to conclude that a self-consistent redetermination of the ground-state and saddle-point deformations would change our calculated energies by less than 0.1 MeV.

These constants (in particular a_0) differ slightly from the preliminary set presented in Ref. [25]. Those constants were affected by an error in the expression for the a_0 energy term in the constant-adjustment program. However, none of the other previous results, conclusions or figures were affected significantly by this computer-program bug. Here we have checked the calculation of macroscopic-model saddle-point shapes and energies by the use of two independently written codes. The microscopic energy model is unchanged from [2].

The 1992 calculation reproduced an experimental 1989 nuclear mass table [26] with a model error of 0.779 MeV, and 28 barrier heights with model error of 1.4 MeV. The revised data set here [4, 5, 27] incorporates seven new experimental barrier heights and removes four old ones. The fit to the revised table of 31 barriers has an rms error of 0.999 MeV, and the fit to the same 1989 mass table has a model error of 0.752 MeV using the parameters in the last column of Table I. We show the experimental and calculated barrier heights as well as remaining discrepancies in Table II and Fig. 3.

This work was supported by the U. S. DOE.

-
- [1] P. Möller and J. R. Nix, *Atomic Data Nucl. Data Tables* **26**, 165 (1981).
[2] P. Möller, J. R. Nix, W. D. Myers, and W. J. Swiatecki, *Atomic Data Nucl. Data Tables* **59**, 185 (1995).
[3] M. A. McMahan, L. G. Moretto, M. L. Padgett, G. J. Wozniak, L. G. Sobotka, and M. G. Mustafa, *Phys. Rev. Lett.* **54**, 1995 (1985).
[4] D. N. Delis, Y. Blumenfeld, D. R. Bowman, N. Colonna, K. Hanold, K. Jing, M. Justice, J. C. Meng, G. F. Peaslee, G. J. Wozniak, and L. G. Moretto, *Nucl. Phys. A* **534**, 403 (1991).
[5] K. X. Jing, L. G. Moretto, A. C. Veeck, N. Colonna, I. Lhenry, K. Tso, K. Hanold, W. Skulski, Q. Sui, and G. J. Wozniak, *Nucl. Phys. A* **645**, 203 (1999).
[6] A. J. Sierk, *Phys. Rev. Lett.* **55**, 582 (1985).
[7] A. J. Sierk, *Phys. Rev. C* **33**, 2039 (1986).
[8] P. Möller and A. Iwamoto, *Phys. Rev. C* **61**, 047602 (2000).
[9] P. Möller, D. G. Madland, A. J. Sierk, and A. Iwamoto, *Nature* **409**, 785 (2001).
[10] W. D. Myers, *Droplet model of atomic nuclei* (IFI/Plenum, New York, 1977).
[11] P. Möller, J. R. Nix, and W. J. Swiatecki, *Nucl. Phys. A* **492**, 349 (1989).
[12] V. Luc and P. Soille, *IEEE Transactions on Pattern Analysis and Machine Intelligence*, **13**, 583 (1991).
[13] A. Mamdouh, J. M. Pearson, M. Rayet, and F. Tondeur, *Nucl. Phys. A* **644**, 389 (1998).
[14] B. Hayes, *Am. Sci.* **88**, 481 (2000).
[15] S. Åberg, H. Flocard, and W. Nazarewicz, *Ann. Rev. Nucl. Sci.* **40**, 439 (1990).
[16] J. L. Egido, L. M. Robledo, and R. R. Chasman, *Phys. Lett. B* **393**, 13 (1997).
[17] J. F. Berger, M. Girod, and D. Gogny, *Nucl. Phys. A* **502**, c85 (1989).
[18] B. A. Nikolaus, T. Hoch, and D. G. Madland, *Phys. Rev. C* **46**, 1757 (1992).
[19] S. Goriely, F. Tondeur, and J. M. Pearson, *At. Data Nucl. Data Tables*, **77**, 311 (2001).
[20] S. Goriely, M. Samyn, P.-H. Heenen, J. M. Pearson, and F. Tondeur *Phys. Rev. C* **66**, 024326 (2002).
[21] J. R. Nix, *Nucl. Phys. A* **130**, 241 (1969).
[22] W. D. Myers and W. J. Swiatecki, *Nucl. Phys. A* **601** (1996) 141.
[23] V. M. Strutinsky, *Nucl. Phys. A* **95**, 420 (1967).
[24] V. M. Strutinsky, *Nucl. Phys. A* **122**, 1 (1968).
[25] Peter Möller, D. G. Madland, A. J. Sierk, and A. Iwamoto, *Proc. International Conference on Nuclear Data for Science and Technology (ND2001)*, October 7–12, Tsukuba, Japan, *Journal of Nuclear Science and Technology*, Supplement 2, 703 (2002).
[26] G. Audi, *Midstream atomic mass evaluation*, private

- communication (1989), with four revisions.
[27] D. G. Madland, Private communication (2001).